



## Review

## Quantifying greenhouse gas emissions from wastewater treatment plants: A critical review

Xinyue He<sup>a</sup>, Haiyan Li<sup>a,\*</sup>, Juanjuan Chen<sup>b</sup>, Huan Wang<sup>c</sup>, Lu Lu<sup>a,\*\*</sup><sup>a</sup> State Key Laboratory of Urban-rural Water Resources and Environment, School of Ecology and Environment, Harbin Institute of Technology, Shenzhen, Shenzhen, 518055, China<sup>b</sup> Guangdong Branch, Beijing General Municipal Engineering Design & Research Institute Co., Ltd, Guangzhou, 510075, China<sup>c</sup> School of Materials and Environmental Engineering, Shenzhen Polytechnic University, Shenzhen, 518055, China

## ARTICLE INFO

## Article history:

Received 19 December 2024

Received in revised form

24 July 2025

Accepted 25 July 2025

## Keywords:

Greenhouse gases

Fossil CO<sub>2</sub>

Measurement techniques

Wastewater treatment

Nationwide emission estimation

## ABSTRACT

Greenhouse gas (GHG) emissions from wastewater treatment plants (WWTPs) are increasingly recognized as significant contributors to anthropogenic climate change, primarily through the release of methane (CH<sub>4</sub>), nitrous oxide (N<sub>2</sub>O), and carbon dioxide (CO<sub>2</sub>). Current research on GHG quantification in WWTPs predominantly relies on estimated emission factors. However, this introduces substantial uncertainties in emission estimates due to limited *in situ* measurements and variability in quantification methods. Here we review advances in GHG measurement techniques, integrating literature data with our *in situ* studies. We show that unit-based methods, such as flux chambers and optical gas imaging, pinpoint emission hotspots in individual processes, while plant-integrated approaches—like tracer gas dispersion, mobile laboratories and aerial surveys—deliver comprehensive plant-scale estimates. These techniques reveal wide variability in emissions, with CH<sub>4</sub> rates spanning 0.04–427 kg h<sup>−1</sup> and N<sub>2</sub>O up to 22.1 kg h<sup>−1</sup>, but most studies are short-term, gas-specific and neglect fossil CO<sub>2</sub>, which can inflate IPCC inventories by up to 22.8 % upon inclusion. Technology- and plant-specific emission factors, calibrated via on-site data, markedly enhance accuracy by accounting for local factors like treatment processes and influent composition. We call for national emission inventories via long-term, multi-gas measurements, guiding targeted mitigation strategies and transforming WWTPs toward carbon-neutral, climate-smart infrastructures.

© 2025 The Authors. Published by Elsevier B.V. on behalf of Chinese Society for Environmental Sciences, Harbin Institute of Technology, Chinese Research Academy of Environmental Sciences. This is an open access article under the CC BY-NC-ND license (<http://creativecommons.org/licenses/by-nc-nd/4.0/>).

## 1. Introduction

Wastewater treatment is a significant yet often overlooked source of anthropogenic greenhouse gas (GHG) emissions, contributing to global climate change in ways that remain inadequately quantified [1–4]. Although it is well understood that methane (CH<sub>4</sub>) is primarily produced by anaerobic microbial activity [5–7] and nitrous oxide (N<sub>2</sub>O) predominantly results from biological and chemical processes [8–10], the complexity of emission sources poses ongoing challenges. These gases can be directly emitted from various treatment units (Fig. 1a) or stripped during aeration; their significant spatiotemporal variability complicates the development of comprehensive sector-wide inventories. Fossil carbon dioxide (CO<sub>2</sub>) is frequently omitted from

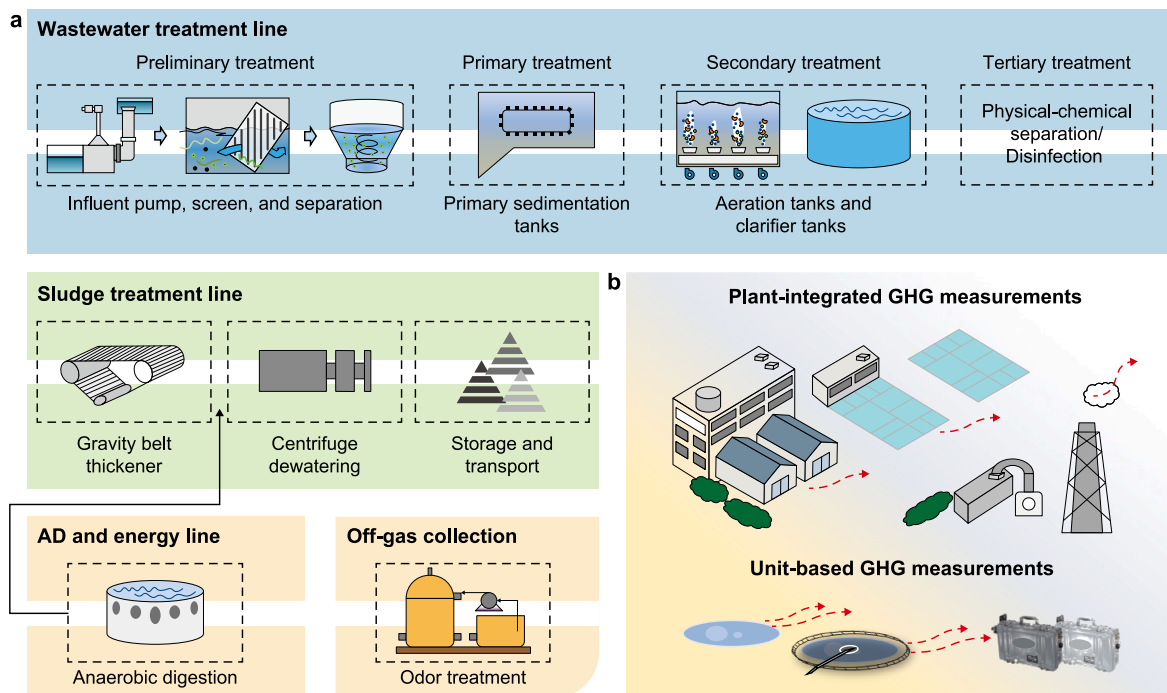
Intergovernmental Panel on Climate Change (IPCC) Scope 1 inventories, although it is recognized as a direct contributor to GHG emissions [11–14]. As a result, quantifications of wastewater GHG emissions are highly uncertain, and emission accounting at the plant, regional, and national scales exhibits substantial variability.

The 2006 IPCC Guidelines for National Greenhouse Gas Inventories and the 2019 Refinement have been widely applied to estimate GHG emissions from wastewater treatment plants (WWTPs) using the emission factor (EF) approach [15,16]. While IPCC methods involve EFs derived from field measurements, past studies have been limited in this regard and lacking consideration of different treatment technologies [17,18]. A study of 63 WWTPs in the United States, conducted from 2019 to 2021, revealed that 71 % of measured CH<sub>4</sub> EFs exceeded the IPCC-recommended upper bounds, leading to annual emission estimates nearly double the IPCC projections [19]. The IPCC EFs have been established primarily based on measurements in developed countries and may not apply to other regions. For example, the CH<sub>4</sub> EF for centralized,

\* Corresponding author.

\*\* Corresponding author.

E-mail addresses: [lihaiyan2021@hit.edu.cn](mailto:lihaiyan2021@hit.edu.cn) (H. Li), [lulu@hit.edu.cn](mailto:lulu@hit.edu.cn) (L. Lu).



**Fig. 1.** **a**, A schematic of a typical wastewater treatment plant with wastewater collection and treatment (wastewater treatment line), sludge treatment (sludge treatment line), energy recovery (anaerobic digestion [AD] and energy line), and off-gas collection and treatment. **b**, Greenhouse gas (GHG) emission measurements for the whole plant using unit-based and plant-integrated methods.

aerobic WWTPs, as given in the 2019 IPCC Refinement guidelines, is around nine times higher than that obtained from field measurements in China [20]. Thus, large discrepancies often occur between the results of IPCC methods and the actual GHG emission levels of WWTPs, and on-site measurements provide more quantitative information on plant-specific GHG emissions [21].

There are two main approaches to measuring GHG emissions from WWTPs: unit-based and plant-integrated measurements (Fig. 1b). Unit-based measurements, such as flux chamber methods [22–24] and optical gas imaging techniques [25,26], target localized emissions from specific processes. These measurements usually involve aggregating the emissions from individual sources to determine a whole plant's emissions. In contrast, plant-integrated measurements enable direct quantification at the plant scale through aerial surveys [27], tracer gas dispersion methods [13,28], or mobile laboratory platforms [19]. Additionally, off-gas measuring techniques for monitoring gas concentrations from exhaust pipelines can be applied to quantify the overall emissions of WWTPs equipped with extensive air collection systems [22,29]. The application of different sampling methods and analytical techniques may lead to significant variabilities in the results obtained, making a systematic evaluation of these methods crucial for selecting appropriate measurement strategies for different WWTP configurations.

Unlike previous studies that primarily focused on specific GHGs, individual monitoring techniques, or technical aspects in isolation [30,31], the present study involved a systematic and comparative assessment of the accuracy, scalability, and practical feasibility of various methods. By evaluating these dimensions using results from the literature and original data, this review moves beyond technical descriptions to actionable insights and recommendations for the real-world implementation of methods for measuring and quantifying CH<sub>4</sub> and N<sub>2</sub>O emissions from WWTPs (Fig. 2). Notably, this review sheds light on the often-

overlooked contributions of fossil CO<sub>2</sub> emissions and the recent advancements made toward their detection and quantification. To enhance the accuracy of emission quantification, technology-specific and plant-specific EF methods are recommended. In summary, this review presents a novel framework for critically evaluating GHG quantification methods in WWTPs, thereby facilitating informed and effective emissions management.

## 2. Methods of data collection

To comprehensively review the GHG emission measurement approaches used in WWTPs, we conducted a structured, keyword-driven literature search in Web of Science, targeting empirical CH<sub>4</sub>, N<sub>2</sub>O, and fossil CO<sub>2</sub> emission datasets derived from field monitoring of wastewater treatment systems from 2000 to 2023. The following search terms were included: Topic search (TS) = ("methane" OR "nitrous oxide" OR "carbon dioxide" OR "fossil carbon dioxide" OR "fossil carbon") and TS = ("wastewater" OR "wastewater treatment" OR "wastewater treatment plant" OR "wwtp") and TS = ("onsite measurement" OR "onsite monitoring" OR "field measurement"). The types of publications included were limited to articles and reviews, focusing exclusively on English-language documents. Following an initial identification and removal of duplicate records, we retained a total of 471 publications. The titles and abstracts of these articles were then screened for relevance, with a particular emphasis on the monitoring techniques applied at full-scale WWTPs and the other key dimensions, including target gas species, emission factors, spatial and temporal resolution, and instrumentation.

## 3. Unit-based measurements for emission quantification

In this section, we summarize the current unit-based techniques for quantifying GHG emissions from individual wastewater

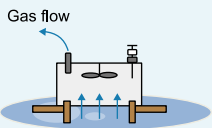
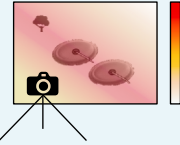
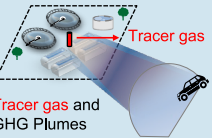
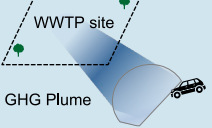
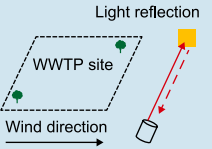

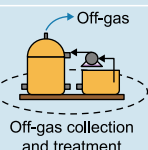
Unit-based methods	Approaches	Main advantages	Major challenges
	<b>Flux chamber (hood) methods (FC)</b> A chamber is placed on the surface of wastewater or sludge treatment units to quantify diffusive GHGs.	<ul style="list-style-type: none"> <li>Localized measurement</li> <li>Long-term observation</li> <li>Portability and flexibility</li> <li>Wide applicability</li> <li>Relatively simple and low cost</li> </ul>	<ul style="list-style-type: none"> <li>Limited spatial coverage</li> <li>Limited to surface emissions</li> <li>Disturbance to working conditions, such as temperature, humidity, and gas exchange, etc.</li> <li>Labor-intensive</li> </ul>
	<b>Optical gas imaging method (OGI)</b> A thermal infrared camera is mainly used to visualize and quantify GHG emissions.	<ul style="list-style-type: none"> <li>Visualization of gas plumes</li> <li>Detection of diffuse or fugitive emissions</li> <li>Non-intrusive at the measurement site</li> <li>Large area coverage</li> </ul>	<ul style="list-style-type: none"> <li>Detection limitations</li> <li>Limited quantification accuracy</li> <li>Sensitivity to meteorological conditions</li> <li>Temperature differential</li> <li>High initial cost</li> <li>Operator expertise required</li> </ul>
Plant-integrated methods	Approaches	Main advantages	Major challenges
	<b>Tracer gas dispersion method (TDM)</b> Controlled release of tracer gas combined with mobile measurement of downwind plumes is used to quantify GHG emissions.	<ul style="list-style-type: none"> <li>High accuracy and precision</li> <li>Effective for large and complex sources</li> <li>Good spatial coverage</li> <li>Flexibility</li> </ul>	<ul style="list-style-type: none"> <li>Limited temporal coverage</li> <li>Sensitivity to meteorological conditions</li> <li>Potential for tracer gas interference</li> <li>Regulatory and permitting requirements, high cost</li> </ul>
	<b>Mobile laboratory method</b> Traversing the entire plume downwind of the sources enables simultaneous real-time monitoring of GHG concentrations.	<ul style="list-style-type: none"> <li>High flexibility and mobility</li> <li>Non-intrusive at the measurement site</li> <li>Good spatial coverage</li> <li>Cost-effective for multiple sites</li> </ul>	<ul style="list-style-type: none"> <li>Limited temporal coverage</li> <li>Sensitivity to meteorological conditions</li> <li>Calibration and validation needs</li> <li>High initial costs</li> </ul>
	<b>Path-integrated optical remote sensing method (PI-ORS)</b> The average GHG concentration along a specific path is measured using light absorption or scattering techniques.	<ul style="list-style-type: none"> <li>High sensitivity and precision</li> <li>Long-term monitoring capability</li> <li>Non-intrusive</li> <li>Large spatial coverage</li> </ul>	<ul style="list-style-type: none"> <li>Complex deployment, and line-of-sight requirement</li> <li>Limited spatial resolution</li> <li>Weather dependence</li> <li>Interference from background sources</li> <li>Calibration and validation needs</li> <li>High cost</li> </ul>
<ul style="list-style-type: none"> <li>Aircraft</li> <li>Drone</li> </ul> 	<b>Aerial surveys (AS)</b> Aircraft or drone equipped with sensors are used to measure atmospheric GHG concentrations over large areas.	<ul style="list-style-type: none"> <li>Wide area coverage</li> <li>High spatial resolution to capture detailed spatial GHG concentrations and identify localized sources of emissions</li> <li>Accessibility to difficult-to-access areas</li> </ul>	<ul style="list-style-type: none"> <li>Complex data processing, and accuracy concerns</li> <li>Time limitations</li> <li>Weather dependence</li> <li>Regulatory and permitting issues</li> <li>High cost, and operator expertise required</li> </ul>
	<b>Off-gas measurements</b> For WWTPs with air collection system	<ul style="list-style-type: none"> <li>High accuracy and precision</li> <li>Long-term monitoring capability</li> </ul>	<ul style="list-style-type: none"> <li>Regulatory and permitting requirements</li> <li>High cost</li> </ul>

Fig. 2. Comparison among different greenhouse gas (GHG) measurement techniques. WWTP: wastewater treatment plant.

treatment units. These details highlight the characteristics and mechanisms of GHG production during wastewater treatment.

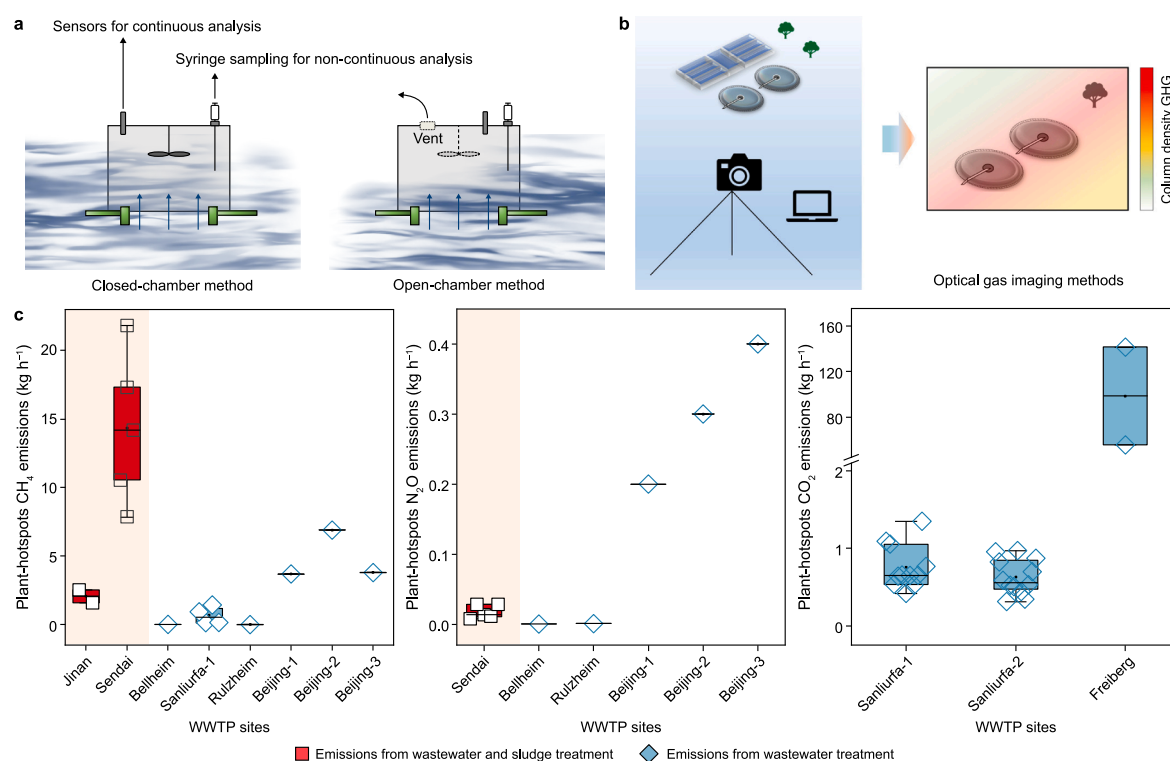
### 3.1. Flux chamber (hood) methods

Flux chamber methods are widely employed to quantify diffusive GHG fluxes across the surfaces of wastewater and sludge treatment units. These methods are of two subtypes based on their application: (a) accumulation closed-chamber methods and (b) flow-through open-chamber methods (Fig. 3a). The former category includes methods that enclose the gases released from relatively static water or solid surfaces within a chamber. The target gas accumulates in a confined environment, and the rate at which its concentration increases is transformed into flux [31]. The concentrations of the trapped airflow at the top of the chamber can be continuously monitored *in situ* using portable gas analyzers. Alternatively, air samples can be drawn using needle-equipped syringes and subsequently analyzed with a gas chromatograph in a specialized laboratory [18,32]. The latter category comprises

methods that allow excess air to escape from the chamber [18,33]. GHG concentrations can be measured in continuous or noncontinuous ways, similar to the above. In the case of aeration tanks, the emission flux is determined by combining the measured concentrations with the aeration rates.

The emission rates of  $\text{CH}_4$ ,  $\text{N}_2\text{O}$ , and  $\text{CO}_2$  from WWTPs are predominantly derived using flux chamber methods, as reported in previous studies (Fig. 3c). Studies focusing solely on wastewater treatment lines have reported  $\text{CH}_4$  emissions ranging from 0.006 to 6.9  $\text{kg h}^{-1}$ . Studies that accounted for WWTPs' total emissions, including GHGs from sludge treatment, have reported a maximum emission rate of 21.8  $\text{kg h}^{-1}$  [18,24,34–36].  $\text{N}_2\text{O}$  emissions remain relatively low across all cases, peaking at around 0.01–0.4  $\text{kg h}^{-1}$  [18,36]. Measurements of  $\text{CO}_2$  emissions from wastewater treatment vary from 0.3 to 141.3  $\text{kg h}^{-1}$  [34,37,38].

Flux chamber methods are frequently used to investigate GHG emissions' spatial and temporal variations and underlying mechanisms in wastewater and sludge treatment units. These chambers are strategically deployed at one or multiple monitoring points to



**Fig. 3.** a–b, Schematic diagram of flux chamber methods (a) and optical gas imaging methods (b). c, CH<sub>4</sub>, N<sub>2</sub>O, and CO<sub>2</sub> emission rates reported in the literature for wastewater treatment with/without sludge treatment units using flux chamber methods. Orange-shaded areas indicate total greenhouse gas (GHG) emissions from wastewater and sludge treatment, while unshaded areas represent wastewater treatment emissions only. The wastewater treatment plants (WWTPs) were sorted in ascending order of treatment capacity (in population equivalent) (Supplementary Table S1–S3).

enable long-term observation. Factors such as operating conditions and water/sludge quality are carefully assessed to identify the causes of peak CH<sub>4</sub> and N<sub>2</sub>O emissions [39,40]. For instance, several studies involving flux chamber methods have shown that GHG emissions from wastewater treatment exhibit distinct seasonal profiles: in summer, the rise in environmental temperature promotes microbial activity, leading to elevated CH<sub>4</sub> production [18,41]. N<sub>2</sub>O emissions peak in winter, and this may be associated with the accumulation of nitrite (NO<sub>2</sub><sup>-</sup>) [18,40]. Nevertheless, it should be noted that flux chamber methods are limited by their constrained coverage of measurement points, and the nonuniform distribution of GHG emissions over the reactor surface may lead to uncertainties in quantification results. Methodological factors, such as the selection of algorithms for various monitoring scenarios and chamber designs [31], are also critical considerations that can influence the accuracy of emissions estimates.

### 3.2. Optical gas imaging methods

Optical gas imaging (OGI) is a method of utilizing thermal infrared cameras to visualize gases. In line with the United States Environmental Protection Agency's recommendations, OGI is used to detect gas leaks in natural gas systems, serving as a tool to guide leak repair (Fig. 3b). Expanding on this, Tauber et al. [42] utilized a nondispersive infrared camera to detect CH<sub>4</sub> emissions from anaerobic digestion systems. Their qualitative assessment involved manholes, concrete cracks, and other forms of leakage, while quantification relied on flux chamber measurements. Recently, a mid-IR ground-based remote sensing technique was used to visualize and quantify GHG emissions [25]. The equipment for this technique included an OGI camera—specifically a mid-infrared (IR) hyperspectral camera weighing about 30 kg—Lidar,

an electrical generator, a weather station, and a field computer. Through the integration of spectroscopic modeling and air motion modeling, the collected visual images and videos were processed to calculate fluxes [25]. This technique was applied at a Sweden WWTP with a biogas production facility, and the total CH<sub>4</sub> and N<sub>2</sub>O emission rates obtained were 10.3 and 1.24 kg h<sup>-1</sup>, respectively.

The OGI method is capable of capturing in detail the variability of CH<sub>4</sub> and N<sub>2</sub>O fluxes through one or more complete operational cycles of a wastewater treatment unit. Moreover, it can effectively identify unknown emission sources, such as unexpected leaks and transient high emissions during sludge loading, even at considerable distances (up to hundreds of meters) from the emission point (s). However, the method's performance is influenced by weather conditions. A temperature difference of at least 1 °C needs to exist between the background temperature and gas temperature to acquire sufficient absorption or emission spectra for quantitative analysis [25].

## 4. Plant-integrated methods for quantifying overall GHG emissions

Plant-integrated measurements are designed to directly quantify total GHG emissions from WWTPs. In most cases, observations of GHG concentrations are interpreted using inverse modeling to estimate emission rates from specific sources. In this section, we discuss the various plant-integrated GHG monitoring techniques reported in the literature.

### 4.1. Tracer gas dispersion method

The tracer gas dispersion method (TDM) relies on the assumption that the target gas and inert tracer gas disperse



similarly in the atmosphere, leading to a stable concentration ratio independent of location [43]. The emission rate of a target gas can be accurately quantified by placing tracer gas cylinders near GHG emission sources and integrating a controlled release of a tracer gas with mobile measurements of downwind plumes (Fig. 4a). This technique has been widely used for quantifying plant-wide emissions in various environments, including farms, landfills, solid waste management facilities, and WWTPs (Fig. 4b).

The plant-wide  $\text{CH}_4$  emission rates of WWTPs have been determined via the TDM in previous studies (Fig. 4c), with values ranging from 1.1 to 103.2  $\text{kg h}^{-1}$ . The records of abnormally high emissions are mainly due to operational issues at the plants. For instance, the high  $\text{CH}_4$  emission rate of 92.3  $\text{kg h}^{-1}$  at the Avedøre WWTP resulted from biogas leakage [13]. Significant  $\text{CH}_4$  emission levels have also been caused by the suboptimal management of treatment processes. For example, the maximum  $\text{CH}_4$  emission rate from open-air sludge stockpiles at the Sweden WWTP was recorded at 22.5  $\text{kg h}^{-1}$ , accounting for 67 % of the total emissions from the plant [28]. In contrast, the relatively low overall emissions recorded at the Lundtofte and Lynetten WWTPs were because the enclosed biosolids facilities could prevent fugitive  $\text{CH}_4$  emissions [43]. A case study at the Mexico WWTP similarly found that poor operational practices in managing primary sludge resulted in plant-wide  $\text{CH}_4$  emissions as high as 52.9  $\text{kg h}^{-1}$  [44].

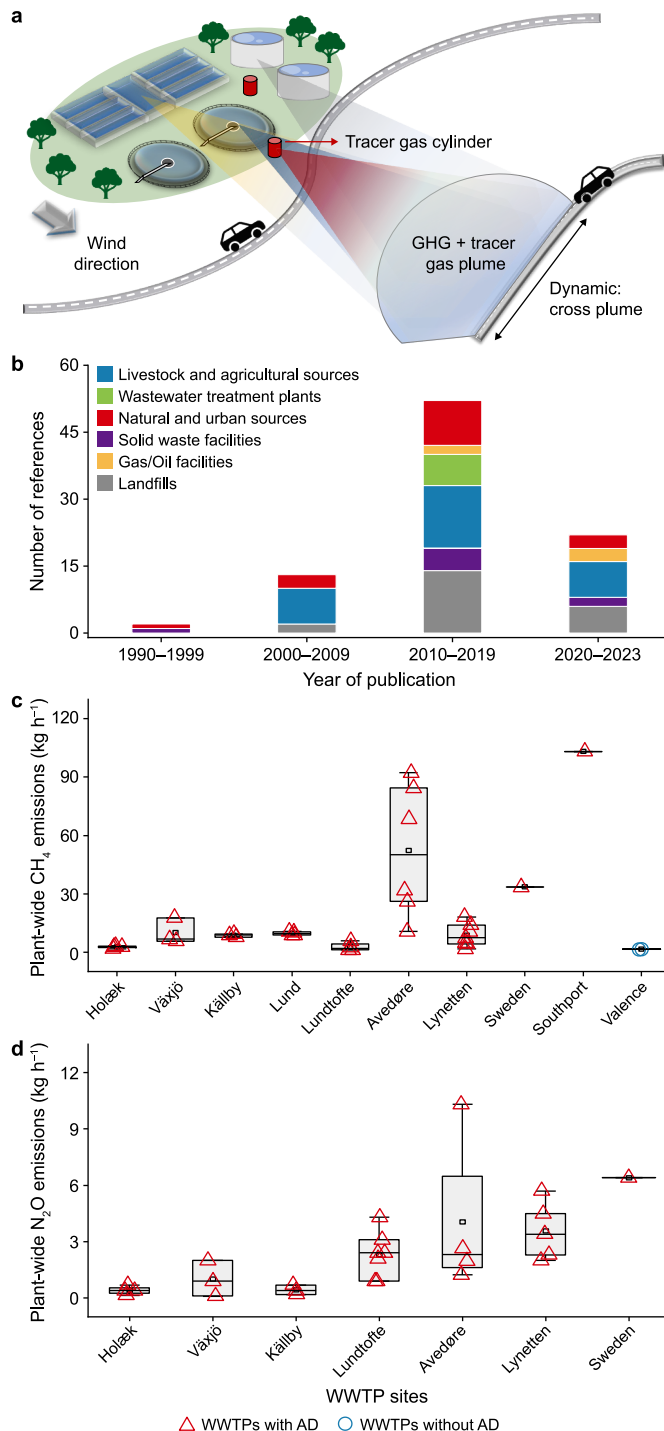
Plant-integrated  $\text{N}_2\text{O}$  emission rates vary from 0.1 to 10.3  $\text{kg h}^{-1}$  (Fig. 4d), largely due to factors such as pollution loads, operational conditions, and climatic conditions [13,28,45]. For example, the highest  $\text{N}_2\text{O}$  emission rate (10.3  $\text{kg h}^{-1}$ ) observed at the Avedøre WWTP was due to elevated  $\text{NO}_3^-$  levels during the monitoring periods [13].

Compared to other techniques, the TDM method allows for accurate quantifications of plant-wide emissions, as it involves determining the quantity of a target gas based on the released amount of a tracer gas. However, the effective implementation of this method requires overcoming several challenges, such as site accessibility, technical requirements, and time investment. First, it is essential to get permission from WWTPs and other associated departments for regulatory compliance and the proper deployment of tracer gas release. Second, the release of the tracer gas has to be precise to guarantee its thorough integration with the target gas. Any oversight in this regard may result in erroneous outcomes. Third, traversing plumes for downwind monitoring campaigns often demands a substantial time commitment, ranging from tens of minutes to several hours. Therefore, the TDM method is less suitable for examining temporal trends in GHG emissions or for long-term applications.

#### 4.2. Mobile laboratory method

GHG emissions can also be quantified by utilizing a mobile laboratory platform that includes trace gas analyzers, weather stations, and global positioning system (GPS), all mounted on an electric vehicle. This kind of platform is specifically designed to traverse entire plumes downwind of emission sources and thereby facilitate simultaneous real-time monitoring of GHG concentrations. By integrating observational data with models that incorporate meteorological conditions, topography, and transport processes, it is feasible to determine the intensity of GHG emissions from a specific source. For instance, Moore et al. [19] applied the mobile laboratory to quantify plant-scale  $\text{CH}_4$  emissions from 63 WWTPs using inverse Gaussian dispersion modeling and Bayesian source rate inference. Over 1000 transects of instantaneous  $\text{CH}_4$  plumes were captured, resulting in plant-averaged  $\text{CH}_4$  emission rates of 0.04–269.3  $\text{kg h}^{-1}$ .

The mobile laboratory approach holds great potential for



**Fig. 4.** **a**, A brief illustration of the tracer gas dispersion method (TDM). **b**, An overview of the TDM applied in different environments. **c–d**, Plant-integrated  $\text{CH}_4$  (**c**) and  $\text{N}_2\text{O}$  (**d**) emission rates from wastewater treatment plants (WWTPs). The measurements used the same tracer gas ( $\text{C}_2\text{H}_2$ ) and gas analyzer (cavity ring-down spectroscopy analyzer). The WWTPs were sorted in ascending order of treatment capacity (in population equivalent) (Supplementary Table S4–S5 and Fig. S1–S2). AD: anaerobic digestion.

assessing GHG emissions from large-scale facilities due to its high mobility and rapid data acquisition capabilities. Compared to the TDM, this approach involves simple procedures and does not require permission for any tracer gas deployment. However, the mobile laboratory approach may lead to higher uncertainties than

the TDM due to atmospheric variability and modeling complexities. To address this challenge, Moore et al. [19] conducted a controlled CH<sub>4</sub> release experiment to compare various approaches to the dispersion model inversion of emission sources. The authors ultimately selected the single-source dispersion model due to its computational efficiency, statistical equivalence to multi-source models, and operational robustness [19].

#### 4.3. Path-integrated optical remote sensing

Path-integrated optical remote sensing (PI-ORS; [Supplementary Fig. S3](#)), a method proposed by the United States Environmental Protection Agency, is used to quantify fugitive pollutant emissions. This method often involves the use of a monitoring strategy with non-intersecting multiple-beam paths, such as open-path Fourier transform infrared spectroscopy (OP-FITIR) or open-path tunable diode laser spectroscopy (OPL), along with retroreflectors, a weather station, and a laptop for measurements. During measurements, a light beam emitted from the OP-FITIR or OPL instrument traverses the open path downwind of the target emission source and reaches a retroreflector. Real-time monitoring of the concentration of a target gas is achieved by measuring the extent to which light is absorbed by the target gas during traversal. Micro-meteorological methods, such as inverse dispersion modeling, can be integrated with PI-ORS to further facilitate the quantification of emission fluxes.

PI-ORS has been extensively applied in previous studies to quantify trace gas emission rates from various sources, especially livestock and agricultural sources and waste treatment facilities ([Supplementary Fig. S3](#)). This method enables the autonomous and remote operation of devices with minimal human intervention and reduced maintenance costs. Moreover, OPL and OP-FITIR support high-frequency quantification of GHG emission rates (e. g., every 10 or 30 min), with monitoring durations lasting up to tens of hours or longer [46]. This method's application in WWTPs is quite limited, and it has been used only in one study to obtain OPL measurements at two WWTPs (with AD) in Switzerland; the average CH<sub>4</sub> emission rates were 0.82 and 0.61 kg h<sup>-1</sup> [47]. This limitation may be attributed to the fact that, compared to other emission sources in rural areas, WWTPs are typically situated in urban areas with limited space, posing which makes it challenges difficult to identifying suitable locations for installing PI-ORS equipment to detect reflections.

#### 4.4. Aerial surveys

Aerial surveys, which utilize aircraft or unmanned aerial vehicles (UAVs), are essential for airborne reconnaissance and monitoring. Aircraft-based approaches are widely adopted for GHG monitoring over extensive areas, and they contribute to enhancing the accuracy of top-down inventories [27,48]. Aircraft-based measurements have recently been applied to estimate CH<sub>4</sub> emissions from intensive sources, including WWTPs [49]. These flight experiments were conducted at four WWTPs and involved a light aircraft equipped with GPS systems, air turbulence probes, and trace gas analyzer instruments. The aircraft followed closed-loop flight paths around each plant, gradually ascending to an altitude above a GHG plume. The CH<sub>4</sub> emission rates were quantified based on mass balance principles and Gauss's law. The results revealed varying emission rates: 204–427 kg h<sup>-1</sup> at the San Jose Santa Clara WWTP, 82–130 kg h<sup>-1</sup> at the East Bay Municipal Utility District Oakland WWTP, 62–229 kg h<sup>-1</sup> at the San Francisco Southeast WWTP, and 120 kg h<sup>-1</sup> at the Central Contra Costa WWTP. The application of aerial measurements in WWTPs may be limited by airspace access and technical requirements.

UAVs or drones are flexible monitoring options for *in situ* atmospheric measurements or the remote sensing of GHG concentrations at small, localized sources [50]. Real-time GHG sampling and analysis can be performed using an integrated instrumentation system onboard the drone. Alternatively, air samples can be collected through an onboard gas collection system [51] or pumped to the ground via a tube [52], with subsequent on-site or off-site analyses determining the gas concentrations. A variety of methods, including the mass balance box method and Gaussian plume inversion models, can be used to quantify GHG emission fluxes. For example, CH<sub>4</sub> emissions from a sludge deposit at a WWTP were measured using a sensitive drone system equipped with a CH<sub>4</sub> sensor and quantified using mass balance calculations; the total CH<sub>4</sub> flux was determined to be 7.4 kg h<sup>-1</sup> [26]. Compared to other techniques, the drone-based method has clear advantages in maneuverability, making it uniquely applicable in remote or inaccessible environments as well as for leak detection and mapping. Challenges related to UAV applications include the need to miniaturize high-performance instrumentation and to restrict flight durations to 45 min due to battery constraints. These factors may limit the temporal resolution and continuity of emission monitoring.

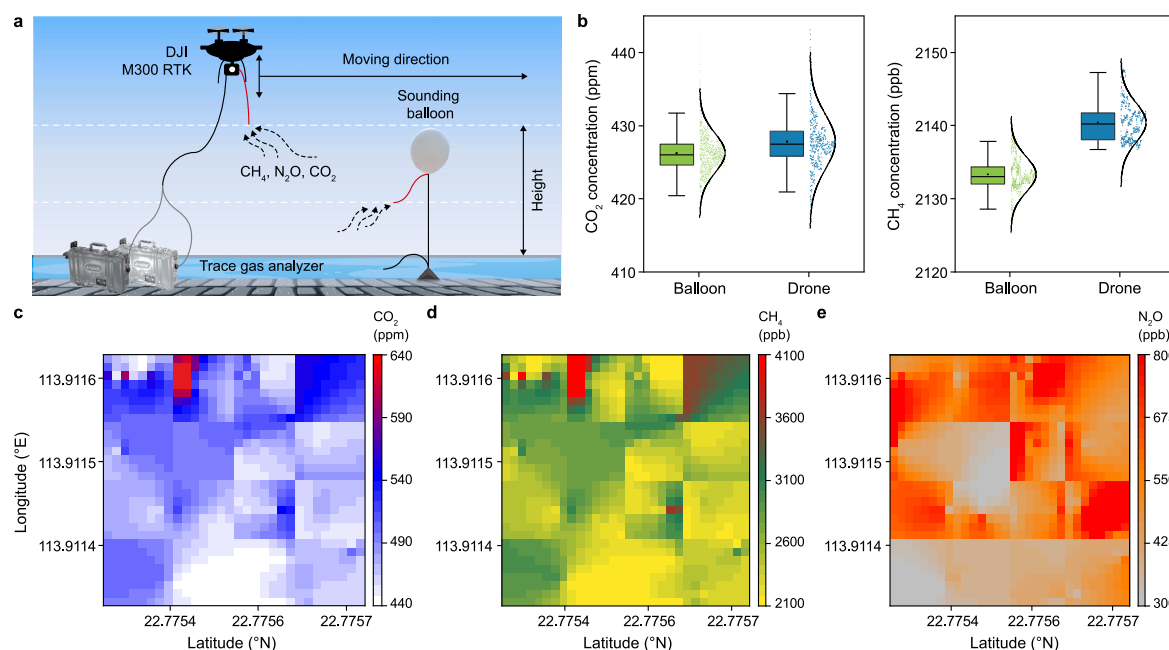
We applied a drone system to map the GHG emission hotspots at a WWTP. Air samples were pumped to the ground via a tube connected to the drone and subsequently measured using ground-based online trace gas analyzers ([Fig. 5a](#)). The sampling inlet was positioned at a distance from the drone to minimize potential interference with the drone's flight during gas sampling. This was confirmed through a comparative experiment using both a drone and a sounding balloon as flight platforms ([Fig. 5b](#)). The drone platform proved effective in visualizing the spatial distribution of the GHG plumes ([Fig. 5c–e](#)). Emission hotspots, such as aeration and anoxic tanks, were clearly observed. The high-emission spots for CH<sub>4</sub> and CO<sub>2</sub> were spatially consistency, while those for N<sub>2</sub>O showed slight deviations.

#### 4.5. Off-gas measurements for plants with air collection systems

An increasing number of WWTPs are being constructed underground or with covered and sealed treatment units to facilitate the centralized collection, treatment, and discharge of exhaust gases [53]. GHG measurements can be conducted at these enclosed plants by directly measuring the GHG concentrations in the exhaust pipelines of the air collection systems through either online monitoring or offline analysis using gas bags. It is feasible to calculate the GHG emissions of an entire plant by incorporating additional parameters, such as gas flow rates.

At the Kralingseveer WWTP (with anaerobic digestion [AD]) in the Netherlands, all process units, except for the secondary settlers, are covered to capture off-gases for treatment. Plant-wide GHG emissions have been estimated at this WWTP via online monitoring, yielding CH<sub>4</sub> emission rates of 8.8–17.9 kg h<sup>-1</sup> and N<sub>2</sub>O emission rates of 2.6–17.7 kg h<sup>-1</sup> [54]. Similarly, the Viikinmäki WWTP (with AD) in Finland, a fully covered underground plant, conducted online monitoring of its exhaust pipeline, which collects off-gases from all units except the dewatered sludge storage. The average N<sub>2</sub>O emission rate was 10.6–22.1 kg h<sup>-1</sup> [29]. Our field experiment at an underground municipal WWTP (without AD) in Guangzhou, China, resulted in average CH<sub>4</sub> and N<sub>2</sub>O emission rates of 1.6 and 0.05 kg h<sup>-1</sup>, respectively [22].

WWTPs equipped with air collection systems stand out as distinctive sewage facilities, well suited to the thorough quantification of plant-wide GHG emissions. In our recent study, the off-gas and unit-based measurements obtained at the aforementioned Guangzhou underground plant (without AD) were



**Fig. 5.** A case study of drone-based mapping of greenhouse gas (GHG) emissions from a wastewater treatment plant (WWTP). **a**, The schematic diagram of the drone-based measurements in this study via a tube connected to the drone and the sounding balloon and using ground-based trace gas analyzers for continuous monitoring. **b**, Comparative analysis of drone and balloon-based platforms for measuring GHG concentrations. The test was conducted at an upwind field with no interference sources. **c–e**, The application of a drone-based monitoring platform for CO<sub>2</sub> (**c**), CH<sub>4</sub> (**d**), and N<sub>2</sub>O (**e**) measurements over a WWTP.

compared to determine the differences in overall GHG emission quantification [22]. Our results revealed that the off-gas measurements were approximately 3–9 times higher than the unit-based measurements. This underscores the limitations of conventional unit-based approaches in capturing total emissions.

A comparative analysis of three fully covered WWTPs—Guangzhou (19,000 m<sup>3</sup> d<sup>−1</sup>, low-strength influent), Viikinmäki (310,000 m<sup>3</sup> d<sup>−1</sup>), and Kralingseveer (50,000–100,000 m<sup>3</sup> d<sup>−1</sup>)—with distinct influent characteristics and treatment configurations has revealed substantial heterogeneity in GHG emissions [22,29,54]. The CH<sub>4</sub> emission rates at the Kralingseveer WWTP, which incorporates advanced sludge-to-energy conversion processes, were 5.5–11.1 times higher than those at the Guangzhou plant, which lacks AD. N<sub>2</sub>O fluxes at the Kralingseveer and Viikinmäki facilities, which had higher overall capacities, were up to two orders of magnitude greater than those at the Guangzhou facility, likely due to higher influent nitrogen loads (i.e., 40–60 mg L<sup>−1</sup> for Kralingseveer and Viikinmäki vs. ~39 mg L<sup>−1</sup> for Guangzhou) and climatic conditions that influence the nitrification-denitrification pathways. These contrasting emission profiles highlight the limitations of applying uniform IPCC emission factors across WWTPs with diverse operational scales and environmental contexts.

#### 4.6. Recommendations for plant-wide GHG emission quantification using on-site measurements

Unit-based methods offer significant advantages for investigating GHG emissions from specific process areas. Flux chamber measurements can be performed in parallel with wastewater sampling and analysis, allowing GHG emission data to directly inform process optimization and adjustments. OGI provides an intuitive visualization of emission sources and their distribution, making it particularly effective for monitoring complex or hard-to-access areas.

However, for plant-wide quantification, plant-integrated measurements are recommended. The mobile laboratory method provides a practical and efficient solution for large-scale emissions assessment in the wastewater treatment sector. In addition, PI-ORS is particularly suitable for the long-term monitoring of individual plants, as its continuous, real-time operations cause minimal disruption to plant operations and enable the detection of emission fluctuations under varying conditions and across different seasons.

When monitoring objectives include both integrated emission quantification and the identification of specific sources, the following techniques are recommended. First, TDM can facilitate the quantification of total plant emissions and also provide insights into the overall distribution and localization of emission sources [28,44]. Second, aircraft surveys can facilitate comprehensive plant-wide emission quantification and hotspot identification. Third, UAV measurements can be valuable in this regard but may face challenges in fully capturing plumes due to plant layout constraints. To enhance measurement accuracy, strategies aimed at (a) capturing full plumes downwind through screen flights and (b) using screen or box flights to quantify emissions from individual treatment units, with aggregated measurements yielding total emissions estimates, can be implemented. Finally, for underground plants or fully covered plants and reactors, off-gas measurements can be used to quantify total emissions in centralized ventilation systems or to assess the source-specific contributions of unit-level exhaust points.

To increase accuracy, we suggest employing a combination of methods for quantifying wastewater GHG emissions. Previously reported plant-wide GHG emissions of various WWTPs, derived from both unit-based and plant-integrated measurements (Fig. 6). Among these, aircraft surveys are associated with the highest median CH<sub>4</sub> emission rate of 121.8 kg h<sup>−1</sup> (Fig. 6a). While this elevated value may partly reflect substantial CH<sub>4</sub> emissions from ADs [49], its marked excess relative to other methods suggests that

aircraft-based measurements may systematically overestimate CH<sub>4</sub> emissions. Flux chamber methods are evidently unsuitable for measuring GHG emissions across entire plants due to their limited coverage of emission sources. Considering the above limitations, the use of different measurement techniques can lead to complementary benefits, resulting in reliable GHG quantification for the development of effective GHG reduction strategies [22,28,44].

The plant-wide N<sub>2</sub>O emissions quantified using the off-gas measurement approach were notably higher than those obtained with other methods (Fig. 6b). This discrepancy likely arises because off-gas measurements directly capture high-concentration releases from emission points, whereas alternative methods may average or miss transient peaks; or because of the large volume of treated wastewater used in the former. Plant-wide N<sub>2</sub>O monitoring has been studied less extensively than CH<sub>4</sub> monitoring, resulting in a limited understanding of N<sub>2</sub>O emission characteristics. Vasilaki et al. [55] reviewed the quantification and mitigation of N<sub>2</sub>O emissions across different process groups, highlighting that insufficient reporting makes it challenging to compare N<sub>2</sub>O emissions across various WWTPs. We encourage researchers to conduct more comprehensive plant-wide N<sub>2</sub>O measurements using established techniques and instruments in the future.

## 5. Fossil CO<sub>2</sub> emissions from wastewater treatment

In this section, we review the distribution of fossil carbon in wastewater, sludge, and gas samples, outlining its fate during the wastewater treatment process. We also discuss our measurements of fossil carbon and fossil CO<sub>2</sub> emissions from wastewater treatment, highlighting the current challenges in this area. There is a data gap in fossil carbon measurements that needs to be filled in order to support the full-scale quantification of GHG emissions from wastewater.

### 5.1. Fossil carbon in wastewater treatment systems

Until the last decade, organic carbon in wastewater was considered wholly biogenic, mainly originating from organic wastes generated by domestic or commercial activities, such as food residuals and human excrement [16]. Wastewater CO<sub>2</sub> emissions were consequently treated as biogenic and omitted from GHG accounting inventories [15]. However, since 2009,

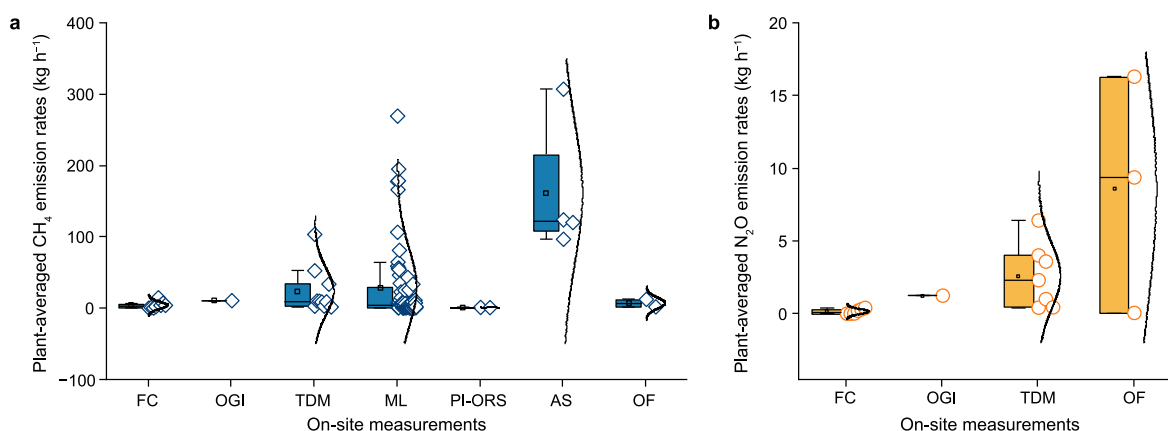
emerging research has highlighted the pervasive presence of fossil organic carbon in wastewater. This is largely attributed to the widespread use of petroleum-based products (e.g., detergents, cosmetics, pharmaceuticals, surfactants, and food additives) in both domestic and commercial settings [11,14]. Surveys have revealed that the presence of fossil organic carbon leads to the release of fossil CO<sub>2</sub> from wastewater systems, contributing to the underestimation of total GHG emissions [12,13,56].

The fossil carbon levels recorded in wastewater, sludge, and gas samples are depicted (Fig. 7). Fossil carbon accounts for about 4–7 % and 8–14 % of WWTP influents from domestic sewage and domestic-industrial mixed wastewater, respectively [14]. In a specific case of municipal influents, the contribution of fossil carbon has reached as high as 28 % [56]. After entering WWTPs, fossil carbon undergoes conversion and migration through three pathways: partial biodegradation into CO<sub>2</sub> and CH<sub>4</sub>, retention in sludge and subsequent digestion to produce CH<sub>4</sub> and CO<sub>2</sub>, or discharge from the plant through excess sludge (treated off-site) and effluent [14,56]. Most of the fossil carbon in influents is transferred to the gas phase and sludge.

In the present study, we collected influent, effluent, and sludge samples from a municipal WWTP in Guangzhou, China, for <sup>14</sup>C measurements using accelerator mass spectrometry (see Section 5.2 for details). The results indicate that the fossil carbon contribution of this WWTP's domestic-industrial mixed wastewater influent was generally lower than those reported in the literature (Fig. 7). In contrast, the sludge biosolids exhibited a notable proportion of fossil carbon, accounting for 21.7 % of the total carbon levels. The difference between the findings of our study and the results reported in the literature may be attributed to influent quality, treatment processes, or effluent quality requirements. Since studies in this field are limited, conducting an in-depth comparison and analysis is challenging.

### 5.2. Identification of fossil carbon via radiocarbon analysis

The quantification of biogenic carbon and fossil carbon relies on radiocarbon (<sup>14</sup>C isotope) analyses. The isotope <sup>14</sup>C is produced naturally through the collision of cosmic rays with nitrogen atoms (<sup>14</sup>N + <sup>1</sup><sub>0</sub>n → <sup>14</sup>C + <sup>1</sup><sub>1</sub>H → oxidized to CO<sub>2</sub>), and it has a half-life of 5700 ± 30 years [57]. In contrast, fossil fuels, which are millions of years old, lack the <sup>14</sup>C isotope signature [58]. Fossil-derived products, such as CO<sub>2</sub> resulting from fossil fuel combustion,



**Fig. 6.** A summary of plant-wide CH<sub>4</sub> (a) and N<sub>2</sub>O (b) emission rates reported in literature obtained through unit-based measurements and plant-integrated measurements. The data points represent the average emission rate of each plant reviewed in the previous sections. FC: flux chamber method; OGI: optical gas imaging method; TDM: tracer gas dispersion method; ML: mobile laboratory method; PI-ORS: path-integrated optical remote sensing method; AS: aerial survey; OF: off-gas measurement method. Among them, FC and OGI belong to the unit-based methods, while others are plant-integrated methods.



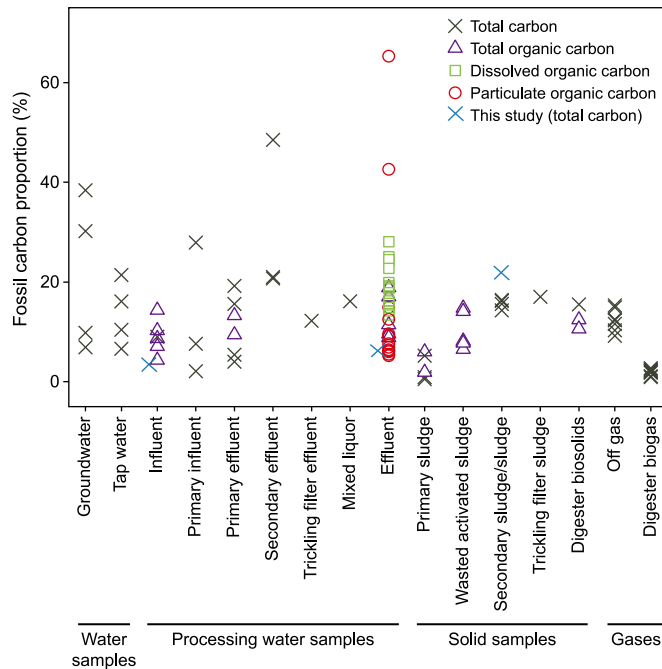


Fig. 7. A summary of fossil carbon proportions in wastewater, sludge, and gas samples based on literature (Supplementary Table S6) and measurements in our study.

predominantly exhibit stable isotope signatures composed of  $^{12}\text{C}$  and  $^{13}\text{C}$ . Thus, radiocarbon  $^{14}\text{C}$  serves as a tracer for bioproducts produced from recent atmospheric  $\text{CO}_2$ .

The ISO 16620-2 standard ("Plastic-determination of bio-based carbon content") lists three methods for determining bio-based carbon content: liquid scintillation counter (LSC), beta-ionization (BI), and accelerator mass spectrometry (AMS). Among these, AMS is the most commonly used due to its relatively short measurement duration and the direct availability of  $^{14}\text{C}$  presence information [14,56]. A detailed calculation procedure based on the AMS method [14] is outlined below.

According to the isotope mixing model,

$$p\text{MC}(s) = \text{REF}_{\text{bio}} \times X_{\text{bio}} + \text{REF}_{\text{ff}} \times X_{\text{ff}} \quad (1)$$

Here, the  $p\text{MC}(s)$  represents the percent modern carbon content of the samples. The measured  $p\text{MC}$  values are dimensionless and expressed in percent units;  $\text{REF}_{\text{bio}}$  and  $\text{REF}_{\text{ff}}$  represent the reference radiocarbon values of biogenic carbon ( $^{14}\text{C}_{\text{bio}}$ ) and fossil fuel carbon ( $^{14}\text{C}_{\text{fossil}}$ ), respectively, measured in  $p\text{MC}$  units;  $X_{\text{bio}}$  and  $X_{\text{ff}}$  are the respective proportions of bio-based and fossil-based carbon content (%), with their total summing up to 100%.

The complete decay of  $^{14}\text{C}$  in fossil fuel carbon results in  $\text{REF}_{\text{ff}} = 0 \text{ pMC}$ . Meanwhile, biogenic carbon consists of isotopic characteristics that remain in equilibrium with the modern atmosphere, denoted as  $\text{REF}_{\text{bio}} = \text{REF}_{\text{atm}}$ . For the year 2020,  $\text{REF}_{\text{atm}}$  was measured at 100.2  $p\text{MC}$ . Therefore, equation (1) can be transformed into equation (2):

$$p\text{MC}(s) = \text{REF}_{\text{atm}} \times X_{\text{bio}} \quad (2)$$

The formula for determining the proportion of bio-based carbon content can be derived as follows:

$$X_{\text{bio}} = \frac{p\text{MC}(s)}{\text{REF}_{\text{atm}}} \times 100\% \quad (3)$$

For instance, an AMS analysis conducted in this study yielded a  $p\text{MC}$  value of  $78.3 \pm 0.3$  for a thickened sludge sample. Using

equation (4),  $X_{\text{bio}}$  was calculated to be 78.3 %. Consequently,  $X_{\text{ff}}$  was determined to be 21.7 %.

$$X_{\text{bio}} = \frac{p\text{MC}(s)}{\text{REF}_{\text{atm}}} \times 100\% = \frac{78.3}{100} \times 100\% = 78.3\% \quad (4)$$

When conducting our measurements, we found that AMS analyzers are not commonly available in standard laboratories because of their high cost and stringent operational requirements. Moreover, there are no established pretreatment protocols for various sample types, and the literature on the fate of fossil carbon during wastewater treatment remains limited.

### 5.3. Fossil $\text{CO}_2$ emissions

Fossil organic carbon in the wastewater leads to fossil  $\text{CO}_2$  emissions during wastewater treatment. Schneider et al. [12] conducted measurements at a Southern California WWTP that mainly receives residential wastewater to identify the hotspot units of fossil  $\text{CO}_2$  emissions. Their observations revealed that the aerobic reactors had the highest fossil  $\text{CO}_2$  flux rates, peaking at  $2.7 \text{ kg h}^{-1}$ , followed by the settling basins at  $0.39 \text{ kg h}^{-1}$  and anoxic reactors at  $0.06 \text{ kg h}^{-1}$ . Regarding the contribution of fossil  $\text{CO}_2$  to total  $\text{CO}_2$  emissions per unit, settling basins had the highest percentage at 66.4 %, followed by aerobic reactors at 34.2 % and anoxic reactors at 11.3 %. Aerobic reactors are major contributors to  $\text{CO}_2$  emissions due to the aerobic biological oxidation of organic matter [38]. A large portion of the produced  $\text{CO}_2$ , including fossil  $\text{CO}_2$ , is directly emitted into the atmosphere, while residual dissolved  $\text{CO}_2$  is gradually released downstream via liquid-phase transport. Notably, although settling basins are characterized by minimal microbial activity, they still exhibit substantial fossil  $\text{CO}_2$  emissions due to their high stripping rates.

In addition to direct measurements of off-gas samples, fossil  $\text{CO}_2$  emissions can be indirectly calculated using the mass balance method. Law et al. [14] used a fossil total organic carbon (TOC) mass balance approach to estimate fossil  $\text{CO}_2$  emissions at four WWTPs. During their secondary treatment process, fossil  $\text{CO}_2$  emissions were calculated at 9.3 and  $2.4 \text{ kg h}^{-1}$  for two plants that exclusively received residential wastewater and at 120.2 and  $122.5 \text{ kg h}^{-1}$  for two plants that received a combination of residential and industrial wastewater.

Law et al. [14] reported that fossil  $\text{CO}_2$  emissions may account for 2–12 % of the total Scope 1 GHG emissions (direct emissions) from wastewater treatment. Tseng et al. [56] further demonstrated that the presence of fossil  $\text{CO}_2$  could elevate total emissions by 12.6 %. Fossil  $\text{CO}_2$  emissions may also arise from on-site and off-site sludge treatment and disposal processes. Biogas resulting from ADs at WWTPs has a low fossil carbon fraction (~3 %; Fig. 7). However, fossil-origin  $\text{CO}_2$  arising from energy recovery through biogas combustion can increase Scope 1 emissions by an additional 10.2 % [56]. Therefore, in systems with on-site energy recovery, the total increase in reported emissions can potentially reach 22.8 %.

For off-site treatment, we consider a case of sludge incineration as an example. According to Zhou et al. [59], China produced 39 million tons of dry sludge annually by 2019, with about 26.7 % undergoing incineration treatment. Assuming a default carbon content of 31 % for dry sludge based on the IPCC guidelines, and considering the fossil carbon proportion of 21.7 % detected in this study, it can be inferred that almost 2.5 million tons of fossil  $\text{CO}_2$  are generated through incineration but are not included in the original IPCC 2019 GHG inventory. There is currently a limited number of studies on fossil  $\text{CO}_2$  emissions from wastewater treatment, which hinders a comprehensive quantification of GHG emissions.

## 6. Nationwide GHG emissions from wastewater treatment in China

The on-site quantification of GHG emissions through direct measurements at WWTPs forms the foundation for nationwide emission estimates using the EF approach. Traditionally, national-scale estimates of wastewater GHG emissions largely relied on the IPCC guidelines. However, the development of various measurement techniques has led to technology-specific and plant-specific EF methods being proposed to reduce estimation uncertainties. In the following section, we use the example of China to illustrate how these methods can be applied to quantify national GHG emissions from wastewater treatment.

### 6.1. IPCC guidelines: applications and future challenges

As the world's largest carbon emitter, China has the most extensive and rapidly expanding wastewater sector [4]. Increasing attention is being paid to assessing the carbon footprints of WWTPs and their impact at the national scale based on the widely adopted IPCC guidelines. The IPCC has provided a well-recognized method for estimating GHG emissions in the wastewater sector. This method integrates activity data—that is, the level of human activities—with EFs that quantify emissions per unit of activity. This tier-based EF approach is designed to accommodate variations in data availability and methodological complexity across different countries and regions.

The IPCC 2006 guidelines have been used in previous studies to quantify GHG emissions from wastewater treatment in China. According to Ma et al.'s [60] estimates, CH<sub>4</sub> emissions from domestic and industrial wastewater treatment increased from 429.9 Mt CO<sub>2</sub>-eq (CO<sub>2</sub>-eq) in 2005 to 592.2 Mt CO<sub>2</sub>-eq in 2010. Ding et al. [61] reported that CH<sub>4</sub> emissions from both types of wastewater treatment rose from 23.7 Mt CO<sub>2</sub>-eq in 1990 to 28.1 Mt CO<sub>2</sub>-eq in 2013. Du et al.'s [62] calculations showed that the national CH<sub>4</sub> emissions from wastewater treatment increased from 357.5 Mt CO<sub>2</sub>-eq in 2000 to 908.9 Mt CO<sub>2</sub>-eq in 2014, with domestic wastewater CH<sub>4</sub> emissions ranging from 64.9 to 336.9 Mt CO<sub>2</sub>-eq. Zhao et al. [63] estimated the CH<sub>4</sub> emissions from wastewater treatment in China based on plant-level data on 2019 municipal WWTPs; the results showed that the total CH<sub>4</sub> emission level was 29.2 Mt CO<sub>2</sub>-eq in 2014. Although many studies used similar statistical sources for activity data, differences in the selection criteria for EFs may lead to large discrepancies in the final emission estimates.

The methodologies and perspectives in the IPCC guidelines are continually refined to narrow the gap between estimated results and actual monitoring data, thereby enhancing the accuracy of emission estimates. In the 2019 Refinement to the 2006 IPCC guidelines for GHG estimation, the EFs of CH<sub>4</sub> for centralized aerobic treatment plants were specified as 0.018 (0.0018–0.054) kg CH<sub>4</sub> per kg biochemical oxygen demand (BOD) based on recent literature, whereas the 2006 IPCC guidelines had set these at 0 for well-managed plants and at 0.18 (0.12–0.24) kg CH<sub>4</sub> per kg BOD for not well-managed plants according to expert judgment. For N<sub>2</sub>O, the plant-level EFs were set at 0.016 (0.00016–0.045) kg N<sub>2</sub>O-N per kg N in the 2019 Refinement and 0.00032 kg N<sub>2</sub>O-N per kg N in the 2006 IPCC guidelines [64]. As a result, the 2006 IPCC guidelines may lead to underestimated CH<sub>4</sub> and N<sub>2</sub>O emissions from wastewater treatment compared to the 2019 Refinement, as revealed in a recent comparison study in Shanghai [65]. The 2019 Refinement still shows substantial deviations from observed values and contains literature citation errors; further refinement is needed for the guidelines to better reflect actual conditions [19,64,66,67]. Future improvements should focus on quantifying nonbiogenic (fossil)

CO<sub>2</sub> emissions from wastewater treatment and discharges.

### 6.2. Technology-specific and plant-specific EF methods

Although the IPCC guidelines have been widely used to quantify GHG emissions from wastewater treatment in China, significant uncertainties exist in these estimates due to the limited availability of *in situ* measurements, insufficient consideration of operational variations across WWTPs, and inherent uncertainties in the published emission factors. Furthermore, the EFs recommended in the IPCC guidelines have primarily been derived from measurements in developed countries and may not apply to developing countries, such as China [20].

Technology-specific EFs have recently been applied to assess GHG emissions from wastewater treatment and improve the accuracy of national emission estimates [4,20,67,68]. Technology-specific EFs are derived from field monitoring activities and categorized by treatment processes and commonly used techniques. For instance, Li et al. [68] developed a plant-level, technology-based CH<sub>4</sub> and N<sub>2</sub>O emission inventory for municipal WWTPs in China, covering 8703 plants and 19 biological treatment technology categories. By combining national and provincial data, the authors estimated that the total CH<sub>4</sub> and N<sub>2</sub>O emissions for 2020 were 41.3 Mt CO<sub>2</sub>-eq and 0.6 Mt CO<sub>2</sub>-eq, respectively [68]. Similarly, Du et al. [4] utilized the activity data of individual municipal WWTPs in China and distinguished EFs according to each plant's treatment processes. The total GHG emissions, including CH<sub>4</sub>, N<sub>2</sub>O, and fossil CO<sub>2</sub>, were calculated to be 53.0 Mt CO<sub>2</sub>-eq in 2019 [4]. These studies reveal substantial spatiotemporal discrepancies in GHG emissions arising from differences in technology preferences across provinces, advancements in wastewater treatment, and shifts in economic and policy conditions.

Several researchers have reported that the plant-specific EF method can be used to achieve accurate emission estimates [19,28]. Plant-level EFs derived from unit-based and plant-integrated measurements—such as those reported by Huang et al. [69], Masuda et al. [18], Samuelsson et al. [28]—are summarized in [Supplementary Table S7](#). Plant-specific EFs vary widely, even among WWTPs with identical treatment technologies. Operational heterogeneity among plants can lead to substantial variations in GHG emissions [28]. Despite its potential, this method has not yet been applied to national-scale emission estimations.

## 7. Conclusion

This study involved a comprehensive review of emission measurements and the quantification of CH<sub>4</sub>, N<sub>2</sub>O, and fossil CO<sub>2</sub> from wastewater treatment. Our comparison of different measurement techniques reveals that flux chamber measurements and the optical gas imaging method offer significant advantages for investigating GHG emissions from individual units. In contrast, the mobile laboratory method and the path-integrated optical remote sensing method are better suited to plant-integrated emission quantification. Tracer gas dispersion, aircraft surveys, and off-gas measurements provide valuable insights into the integrated quantification of emissions from whole plants and the identification of specific sources. However, their applicability may be constrained by the structural characteristics of WWTPs.

Significant levels of fossil carbon, ranging from approximately 4%–28%, have been detected in the WWTP influents. This suggests that fossil CO<sub>2</sub> emissions are released into the atmosphere through the process of biodegradation. Incorporating fossil CO<sub>2</sub> emissions into carbon accounting may increase the original IPCC inventory by up to 22.8%. However, current techniques for detecting fossil

carbon are not easily accessible, and a standardized pretreatment protocol for different types of samples has not been established, highlighting the need for future development in this area.

Researchers have primarily followed the IPCC guidelines to estimate GHG emissions from wastewater treatment at the national scale. However, significant discrepancies may exist between these estimates and the actual emission rates. To address this, a multi-tiered policy framework is essential to enhance GHG monitoring in wastewater management. Standardized protocols should prioritize continuous measurements of CH<sub>4</sub>, N<sub>2</sub>O, and fossil CO<sub>2</sub> at benchmark plants and promote the use of calibrated emission factors for accurate assessments. Real-time GHG concentration data should be integrated with WWTP operational parameters to enable automated verification, thereby facilitating the integrated management of wastewater treatment and GHG emissions. These strategies can collectively address the existing data gaps and support the sector's transition to climate-smart infrastructure.

### CRedit authorship contribution statement

**Xinyue He:** Writing – original draft, Visualization, Methodology, Investigation, Data curation. **Haiyan Li:** Writing – review & editing, Writing – original draft, Supervision, Methodology, Conceptualization. **Juanjuan Chen:** Writing – review & editing. **Huan Wang:** Writing – review & editing. **Lu Lu:** Writing – review & editing, Supervision, Methodology, Conceptualization.

### Data availability

Data can be made available upon reasonable request.

### Declaration of competing interest

The authors declare that they have no known competing financial interests or personal relationships that could have appeared to influence the work reported in this paper.

### Acknowledgements

This work was supported by the National Natural Science Foundation of China (No. 52470071 and 52321005), Shenzhen Science and Technology Program (No. RCBS20210609103731062, KCXST20221021111404011, JCYJ20240813092008011, and KQTD20190929172630447), Scientific Research Project of Shenzhen Polytechnic University (No. 6024310035K) and Natural Science Foundation of Guangdong Province (No. 2021A1515110887 and 2023A1515012063).

### Appendix A. Supplementary data

Supplementary data to this article can be found online at <https://doi.org/10.1016/j.ese.2025.100606>.

### References

- [1] Y. Ou, C. Roney, J. Alsalam, K. Calvin, J. Creason, J. Edmonds, A.A. Fawcett, P. Kyle, K. Narayan, P. O'Rourke, P. Patel, S. Ragnauth, S.J. Smith, H. McJeon, Deep mitigation of CO<sub>2</sub> and non-CO<sub>2</sub> greenhouse gases toward 1.5 °C and 2 °C futures, *Nat. Commun.* 12 (2021), <https://doi.org/10.1038/s41467-021-26509-z>.
- [2] D. Wang, W. Ye, G. Wu, R. Li, Y. Guan, W. Zhang, J. Wang, Y. Shan, K. Hubacek, Greenhouse gas emissions from municipal wastewater treatment facilities in China from 2006 to 2019, *Sci. Data* 9 (2022), <https://doi.org/10.1038/s41597-022-01439-7>.
- [3] L. Lu, J.S. Guest, C.A. Peters, X. Zhu, G.H. Rau, Z.J. Ren, Wastewater treatment for carbon capture and utilization, *Nat. Sustain.* 1 (2018) 750–758, <https://doi.org/10.1038/s41893-018-0187-9>.
- [4] W.-J. Du, J.-Y. Lu, Y.-R. Hu, J. Xiao, C. Yang, J. Wu, B. Huang, S. Cui, Y. Wang, W.-W. Li, Spatiotemporal pattern of greenhouse gas emissions in China's wastewater sector and pathways towards carbon neutrality, *Nat. Water* 1 (2023) 166–175, <https://doi.org/10.1038/s44221-022-00021-0>.
- [5] M. El-Fadel, M. Massoud, Methane emissions from wastewater management, *Environ. Pollut.* 114 (2001) 177–185.
- [6] C. Song, J.-J. Zhu, J.L. Willis, D.P. Moore, M.A. Zondlo, Z.J. Ren, Methane emissions from municipal wastewater collection and treatment systems, *Environ. Sci. Technol.* 57 (2023) 2248–2261, <https://doi.org/10.1021/acs.est.2c04388>.
- [7] R. Ganigué, Z. Yuan, Impact of oxygen injection on CH<sub>4</sub> and N<sub>2</sub>O emissions from rising main sewers, *J. Environ. Manag.* 144 (2014) 279–285, <https://doi.org/10.1016/j.jenvman.2014.04.023>.
- [8] S. Chen, M. Harb, P. Sinha, A.L. Smith, Emerging investigators series: revisiting greenhouse gas mitigation from conventional activated sludge and anaerobic-based wastewater treatment systems, *Environ. Sci.:Water Res. Technol.* 4 (2018) 1739–1758, <https://doi.org/10.1039/c8ew00545a>.
- [9] W. Gruber, P.M. Magyar, I. Mitrovic, K. Zeyer, M. Vogel, L. von Känel, L. Biolley, R.A. Werner, E. Morgenroth, M.F. Lehmann, D. Braun, A. Joss, J. Mohn, Tracing N<sub>2</sub>O formation in full-scale wastewater treatment with natural abundance isotopes indicates control by organic substrate and process settings, *Water Res.* 15 (2022), <https://doi.org/10.1016/j.wroa.2022.100130>.
- [10] D. Caniani, M. Caivano, R. Pascale, G. Bianco, I.M. Mancini, S. Masi, G. Mazzone, M. Firouzian, D. Rosso, CO<sub>2</sub> and N<sub>2</sub>O from water resource recovery facilities: evaluation of emissions from biological treatment, settling, disinfection, and receiving water body, *Sci. Total Environ.* 648 (2019) 1130–1140, <https://doi.org/10.1016/j.scitotenv.2018.08.150>.
- [11] D.R. Griffith, R.T. Barnes, R.P. A. Inputs of fossil carbon from wastewater treatment plants to U.S. rivers and oceans, *Environ. Sci. Technol.* 43 (2009) 5647–5651.
- [12] A.G. Schneider, A. Townsend-Small, D. Rosso, Impact of direct greenhouse gas emissions on the carbon footprint of water reclamation processes employing nitrification–denitrification, *Sci. Total Environ.* 505 (2015) 1166–1173, <https://doi.org/10.1016/j.scitotenv.2014.10.060>.
- [13] H. Yoshida, J. Mønster, C. Scheutz, Plant-integrated measurement of greenhouse gas emissions from a municipal wastewater treatment plant, *Water Res.* 61 (2014) 108–118, <https://doi.org/10.1016/j.watres.2014.05.014>.
- [14] Y. Law, G.E. Jacobsen, A.M. Smith, Z. Yuan, P. Lant, Fossil organic carbon in wastewater and its fate in treatment plants, *Water Res.* 47 (2013) 5270–5281, <https://doi.org/10.1016/j.watres.2013.06.002>.
- [15] D. Bartram, M.D. Short, Y. Ebbe, J. Farkaš, C. Gueguen, G.M. Peters, N. M. Zanzottera, M. Karthik, 2019 Refinement to the 2006 IPCC Guidelines for National Greenhouse Gas Inventories, Volume 5: Waste. Chapter 6: Wastewater Treatment and Discharge, Intergovernmental Panel on Climate Change, 2019.
- [16] M.R.J. Doorn, S. Towprayoon, S.M.M. Vieira, W. Irving, C. Palmer, R. Pipatti, C. Wang, 2006 IPCC Guidelines for National Greenhouse Gas Inventories, 5, Intergovernmental Panel on Climate Change, Waste, 2006. Chapter 6: Wastewater treatment and discharge.
- [17] Y. Wang, X. Lin, D. Zhou, L. Ye, H. Han, C. Song, Nitric oxide and nitrous oxide emissions from a full-scale activated sludge anaerobic/anoxic/oxic process, *Chem. Eng. J.* 289 (2016) 330–340, <https://doi.org/10.1016/j.cej.2015.12.074>.
- [18] S. Masuda, S. Suzuki, I. Sano, Y.-Y. Li, O. Nishimura, The seasonal variation of emission of greenhouse gases from a full-scale sewage treatment plant, *Chemosphere* 140 (2015) 167–173, <https://doi.org/10.1016/j.chemosphere.2014.09.042>.
- [19] D.P. Moore, N.P. Li, L.P. Wendt, S.R. Castañeda, M.M. Falinski, J.-J. Zhu, C. Song, Z.J. Ren, M.A. Zondlo, Underestimation of sector-wide methane emissions from United States wastewater treatment, *Environ. Sci. Technol.* 57 (2023) 4082–4090, <https://doi.org/10.1021/acs.est.2c05373>.
- [20] H. Hua, S. Jiang, Z. Yuan, X. Liu, Y. Zhang, Z. Cai, Advancing greenhouse gas emission factors for municipal wastewater treatment plants in China, *Environ. Pollut.* 295 (2022), <https://doi.org/10.1016/j.envpol.2021.118648>.
- [21] A. Gore, Measure emissions to manage emissions, *Science* 378 (2022) 455.
- [22] Y. Chong, H. Li, T. Pan, L. You, H. Du, B. Yu, J. Chen, N. Ren, L. Lu, More applicable quantification of non-CO<sub>2</sub> greenhouse gas emissions from wastewater treatment plants by on-site plant-integrated measurements, *Sci. Total Environ.* 929 (2024), <https://doi.org/10.1016/j.scitotenv.2024.172598>.
- [23] A. Willén, L. Rodhe, M. Pell, H. Jönsson, Nitrous oxide and methane emissions during storage of dewatered digested sewage sludge, *J. Environ. Manag.* 184 (2016) 560–568, <https://doi.org/10.1016/j.jenvman.2016.10.025>.
- [24] A. Tumendelger, Z. Alshboul, A. Lorke, Methane and nitrous oxide emission from different treatment units of municipal wastewater treatment plants in Southwest Germany, *PLoS One* 14 (2019), <https://doi.org/10.1371/journal.pone.0209763>.
- [25] M. Gållfalk, S.N. Pålédal, R. Sehlén, D. Bastviken, Ground-based remote sensing of CH<sub>4</sub> and N<sub>2</sub>O fluxes from a wastewater treatment plant and nearby biogas production with discoveries of unexpected sources, *Environ. Res.* 204 (2022), <https://doi.org/10.1016/j.envres.2021.111978>.
- [26] M. Gållfalk, S. Nilsson Pålédal, D. Bastviken, Sensitive drone mapping of methane emissions without the need for supplementary ground-based measurements, *ACS Earth Space Chem.* 5 (2021) 2668–2676, <https://doi.org/10.1021/acsearthspacechem.1c00106>.
- [27] B.K. Lamb, M.O.L. Cambaliza, K.J. Davis, S.L. Edburg, T.W. Ferrara,



- C. Floerchinger, A.M.F. Heimbürger, S. Herndon, T. Lauvaux, T. Lavoie, D. R. Lyon, N. Miles, K.R. Prasad, S. Richardson, J.R. Roscioli, O.E. Salmon, P. B. Shepson, B.H. Strim, J. Whetstone, Direct and indirect measurements and modeling of methane emissions in Indianapolis, Indiana, *Environ. Sci. Technol.* 50 (2016) 8910–8917, <https://doi.org/10.1021/acs.est.6b01198>.
- [28] J. Samuelsson, A. Delre, S. Tumlin, S. Hadi, B. Offerle, C. Scheutz, Optical technologies applied alongside on-site and remote approaches for climate gas emission quantification at a wastewater treatment plant, *Water Res.* 131 (2018) 299–309, <https://doi.org/10.1016/j.watres.2017.12.018>.
- [29] H. Kosonen, M. Heinonen, A. Mikola, H. Haimi, M. Mulas, F. Corona, R. Vahala, Nitrous oxide production at a fully covered wastewater treatment plant: results of a long-term online monitoring campaign, *Environ. Sci. Technol.* 50 (2016) 5547–5554, <https://doi.org/10.1021/acs.est.5b04466>.
- [30] D. Ddiba, M. Rahmati Abkenar, C. Liera, Methods for measuring greenhouse gas emissions from sanitation and wastewater management systems: a review of method features, past applications and facilitating factors for researchers, practitioners and other stakeholders, *SIWI Rep* (2024), <https://doi.org/10.51414/sei2024.030>.
- [31] V. Parravicini, A. Filali, A. Delre, O. Gutierrez, H. Duan, Quantification and modelling of fugitive greenhouse gas emissions from urban water systems. Chapter 5: Full-Scale Quantification of N<sub>2</sub>O and CH<sub>4</sub> Emissions from Urban Water Systems, IWA Publishing, 2022, [https://doi.org/10.2166/9781789060461\\_91](https://doi.org/10.2166/9781789060461_91).
- [32] L.T. Huynh, H. Harada, S. Fujii, L.P.H. Nguyen, T.-H.T. Hoang, H.T. Huynh, Greenhouse gas emissions from blackwater septic systems, *Environ. Sci. Technol.* 55 (2021) 1209–1217, <https://doi.org/10.1021/acs.est.0c03418>.
- [33] C.E. Yver Kwok, D. Müller, C. Caldwell, B. Lebègue, J.G. Münster, C.W. Rella, C. Scheutz, M. Schmidt, M. Ramonet, T. Warneke, G. Broquet, P. Ciais, Methane emission estimates using chamber and tracer release experiments for a municipal waste water treatment plant, *Atmos. Meas. Tech.* 8 (2015) 2853–2867, <https://doi.org/10.5194/amt-8-2853-2015>.
- [34] P. Yapiçioğlu, Ö. Demir, Minimizing greenhouse gas emissions of an industrial wastewater treatment plant in terms of water–energy nexus, *Appl. Water Sci.* 11 (2021), <https://doi.org/10.1007/s13201-021-01484-4>.
- [35] J. Wang, J. Zhang, H. Xie, P. Qi, Y. Ren, Z. Hu, Methane emissions from a full-scale A/A/O wastewater treatment plant, *Bioresour. Technol.* 102 (2011) 5479–5485, <https://doi.org/10.1016/j.biortech.2010.10.090>.
- [36] X. Yan, L. Li, J. Liu, Characteristics of greenhouse gas emission in three full-scale wastewater treatment processes, *J. Environ. Sci.* 26 (2014) 256–263, [https://doi.org/10.1016/S1001-0742\(13\)60429-5](https://doi.org/10.1016/S1001-0742(13)60429-5).
- [37] Ö. Demir, P. Yapiçioğlu, Investigation of GHG emission sources and reducing GHG emissions in a municipal wastewater treatment plant, *Greenhouse Gases: Sci. Technol.* 9 (2019) 948–964, <https://doi.org/10.1002/ghg.1912>.
- [38] P. Kosse, T. Kleeberg, M. Lübken, J. Matschullat, M. Wichern, Quantifying direct carbon dioxide emissions from wastewater treatment units by nondispersive infrared sensor (NDIR) – a pilot study, *Sci. Total Environ.* 633 (2018) 140–144, <https://doi.org/10.1016/j.scitotenv.2018.03.174>.
- [39] A. Rodriguez-Caballero, I. Aymerich, M. Poch, M. Pijuan, Evaluation of process conditions triggering emissions of green-house gases from a biological wastewater treatment system, *Sci. Total Environ.* 493 (2014) 384–391, <https://doi.org/10.1016/j.scitotenv.2014.06.015>.
- [40] W. Gruber, K. Villez, M. Kipf, P. Wunderlin, H. Siegrist, L. Vogt, A. Joss, N<sub>2</sub>O emission in full-scale wastewater treatment: proposing a refined monitoring strategy, *Sci. Total Environ.* 699 (2020), <https://doi.org/10.1016/j.scitotenv.2019.134157>.
- [41] S. Masuda, I. Sano, T. Hojo, Y.-Y. Li, O. Nishimura, The comparison of greenhouse gas emissions in sewage treatment plants with different treatment processes, *Chemosphere* 193 (2018) 581–590, <https://doi.org/10.1016/j.chemosphere.2017.11.018>.
- [42] J. Tauber, V. Parravicini, K. Svandal, J. Krampe, Quantifying methane emissions from anaerobic digesters, *Water Sci. Technol.* 80 (2019) 1654–1661, <https://doi.org/10.2166/wst.2019.415>.
- [43] A. Delre, J. Münster, C. Scheutz, Greenhouse gas emission quantification from wastewater treatment plants, using a tracer gas dispersion method, *Sci. Total Environ.* 605–606 (2017) 258–268, <https://doi.org/10.1016/j.scitotenv.2017.06.177>.
- [44] A. Noyola, M.G. Paredes, L.P. Güereca, L.T. Molina, M. Zavala, Methane correction factors for estimating emissions from aerobic wastewater treatment facilities based on field data in Mexico and on literature review, *Sci. Total Environ.* 639 (2018) 84–91, <https://doi.org/10.1016/j.scitotenv.2018.05.111>.
- [45] A. Delre, J. Münster, J. Samuelsson, A.M. Fredenslund, C. Scheutz, Emission quantification using the tracer gas dispersion method: the influence of instrument, tracer gas species and source simulation, *Sci. Total Environ.* 634 (2018) 59–66, <https://doi.org/10.1016/j.scitotenv.2018.03.289>.
- [46] P. Siozos, G. Psyllakis, M. Velegarakis, Remote operation of an open-path, laser-based instrument for atmospheric CO<sub>2</sub> and CH<sub>4</sub> monitoring, *Photonics* 10 (2023), <https://doi.org/10.3390/photonics10040386>.
- [47] M. Bühler, C. Häni, C. Ammann, S. Brönnimann, T. Kupper, Using the inverse dispersion method to determine methane emissions from biogas plants and wastewater treatment plants with complex source configurations, *Atmos. Environ.* X 13 (2022), <https://doi.org/10.1016/j.aeaoa.2022.100161>.
- [48] A.K. Thorpe, C. O'Handley, G.D. Emmitt, P.L. DeCola, F.M. Hopkins, V. Yadav, A. Guha, S. Newman, J.D. Herner, M. Falk, R.M. Duren, Improved methane emission estimates using AVIRIS-NG and an Airborne Doppler Wind Lidar, *Remote Sens. Environ.* 266 (2021), <https://doi.org/10.1016/j.rse.2021.112681>.
- [49] A. Guha, S. Newman, D. Fairley, T.M. Dinh, L. Duca, S.C. Conley, M.L. Smith, A. K. Thorpe, R.M. Duren, D.H. Cusworth, K.T. Foster, M.L. Fischer, S. Jeong, N. Yesiller, J.L. Hanson, P.T. Martien, Assessment of regional methane emission inventories through airborne quantification in the San Francisco Bay area, *Environ. Sci. Technol.* 54 (2020) 9254–9264, <https://doi.org/10.1021/acs.est.0c01212>.
- [50] J.T. Shaw, A. Shah, H. Yong, G. Allen, Methods for quantifying methane emissions using unmanned aerial vehicles: a review, *Philos. Trans. R. Soc. A* 379 (2021), <https://doi.org/10.1098/rsta.2020.0450>.
- [51] W. Chen, Y. Zou, W. Mo, D. Di, B. Wang, M. Wu, Z. Huang, B. Hu, Onsite identification and spatial distribution of air pollutants using a drone-based solid-phase microextraction array coupled with portable gas chromatography-mass spectrometry via continuous-airflow sampling, *Environ. Sci. Technol.* 56 (2022) 17100–17107, <https://doi.org/10.1021/acs.est.2c05259>.
- [52] J.H. Scheller, M. Mastepanov, T.R. Christensen, Toward UAV-based methane emission mapping of arctic terrestrial ecosystems, *Sci. Total Environ.* 819 (2022), <https://doi.org/10.1016/j.scitotenv.2022.153161>.
- [53] A. Talaiekhazani, M. Bagheri, A. Goli, M.R. Talaie Khoozani, An overview of principles of odor production, emission, and control methods in wastewater collection and treatment systems, *J. Environ. Manag.* 170 (2016) 186–206, <https://doi.org/10.1016/j.jenvman.2016.01.021>.
- [54] M.R.J. Daelman, E.M. van Voorthuizen, L.G.J.M. van Dongen, E.I.P. Volcke, M.C. M. van Loosdrecht, Methane and nitrous oxide emissions from municipal wastewater treatment – results from a long-term study, *Water Sci. Technol.* 67 (2013) 2350–2355, <https://doi.org/10.2166/wst.2013.109>.
- [55] V. Vasilaki, T.M. Massara, P. Stanchev, F. Fatone, E. Katsou, A decade of nitrous oxide (N<sub>2</sub>O) monitoring in full-scale wastewater treatment processes: a critical review, *Water Res.* 161 (2019) 392–412, <https://doi.org/10.1016/j.watres.2019.04.022>.
- [56] L.Y. Tseng, A.K. Robinson, X. Zhang, X. Xu, J. Southon, A.J. Hamilton, R. Sobhani, M.K. Stenstrom, D. Rosso, Identification of preferential paths of fossil carbon within water resource recovery facilities via radiocarbon analysis, *Environ. Sci. Technol.* 50 (2016) 12166–12178, <https://doi.org/10.1021/acs.est.6b02731>.
- [57] M.L. Roberts, J.R. Southon, A preliminary determination of the absolute <sup>14</sup>C/<sup>12</sup>C ratio of OX-I, *Radiocarbon* 49 (2016) 441–445, <https://doi.org/10.1017/s003822200042363>.
- [58] H.D. Graven, Impact of fossil fuel emissions on atmospheric radiocarbon and various applications of radiocarbon over this century, *Proc. Natl. Acad. Sci. USA* 112 (2015) 9542–9545, <https://doi.org/10.1073/pnas.1504467112>.
- [59] X. Zhou, J. Yang, X. Zhao, Q. Dong, X. Wang, L. Wei, S.-S. Yang, H. Sun, N.-Q. Ren, S. Bai, Towards the carbon neutrality of sludge treatment and disposal in China: a nationwide analysis based on life cycle assessment and scenario discovery, *Environ. Int.* 174 (2023), <https://doi.org/10.1016/j.envint.2023.107927>.
- [60] Z.-Y. Ma, P. Feng, Q.-X. Gao, Y.-N. Lu, J.-R. Liu, W.-T. Li, CH<sub>4</sub> emissions and reduction potential in wastewater treatment in China, *Adv. Clim. Change Res.* 6 (2015) 216–224, <https://doi.org/10.1016/j.accre.2015.11.006>.
- [61] T. Ding, Y. Ning, Y. Zhang, Estimation of greenhouse gas emissions in China 1990–2013, *Greenhouse Gases Sci. Technol.* 7 (2017) 1097–1115, <https://doi.org/10.1002/ghg.1718>.
- [62] M. Du, Q. Zhu, X. Wang, P. Li, B. Yang, H. Chen, M. Wang, X. Zhou, C. Peng, Estimates and predictions of methane emissions from wastewater in China from 2000 to 2020, *Earths Future* 6 (2018) 252–263, <https://doi.org/10.1002/2017ef000673>.
- [63] X. Zhao, X.K. Jin, W. Guo, C. Zhang, Y.L. Shan, M.X. Du, M.R. Tillotson, H. Yang, X.W. Liao, Y.P. Li, China's urban methane emissions from municipal wastewater treatment plant, *Earths Future* 7 (2019) 480–490, <https://doi.org/10.1029/2018ef001113>.
- [64] W. Gruber, L. von Känel, L. Vogt, M. Luck, L. Biolley, K. Feller, A. Moosmann, N. Krähenbühl, M. Kipf, R. Loosli, M. Vogel, E. Morgenroth, D. Braun, A. Joss, Estimation of countrywide N<sub>2</sub>O emissions from wastewater treatment in Switzerland using long-term monitoring data, *Water Res.* 13 (2021), <https://doi.org/10.1016/j.wroa.2021.100122>.
- [65] J. Xi, H. Gong, Y. Zhang, X. Dai, L. Chen, The evaluation of GHG emissions from Shanghai municipal wastewater treatment plants based on IPCC and operational data integrated methods (ODIM), *Sci. Total Environ.* 797 (2021), <https://doi.org/10.1016/j.scitotenv.2021.148967>.
- [66] D. de Haas, J. Andrews, Nitrous oxide emissions from wastewater treatment – revisiting the IPCC 2019 refinement guidelines, *Environ. Chall.* 8 (2022), <https://doi.org/10.1016/j.envc.2022.100557>.
- [67] C. Song, J.-J. Zhu, J.L. Willis, D.P. Moore, M.A. Zondlo, Z.J. Ren, Oversimplification and misestimation of nitrous oxide emissions from wastewater treatment plants, *Nat. Sustain.* (2024), <https://doi.org/10.1038/s41893-024-01420-9>.
- [68] H. Li, L. You, H. Du, B. Yu, L. Lu, B. Zheng, Q. Zhang, K. He, N. Ren, Methane and nitrous oxide emissions from municipal wastewater treatment plants in China: a plant-level and technology-specific study, *Environ. Sci. Ecotechnol.* 20 (2024), <https://doi.org/10.1016/j.jese.2023.100345>.
- [69] K.-L. Hwang, C.-H. Bang, K.-D. Zoh, Characteristics of methane and nitrous oxide emissions from the wastewater treatment plant, *Bioresour. Technol.* 214 (2016) 881–884, <https://doi.org/10.1016/j.biortech.2016.05.047>.